

See discussions, stats, and author profiles for this publication at: <https://www.researchgate.net/publication/228599631>

# Sorption Kinetics of Hexadecyltrimethylammonium on Natural Clinoptilolite

ARTICLE *in* LANGMUIR · SEPTEMBER 1999

Impact Factor: 4.46 · DOI: 10.1021/la981535x

---

CITATIONS

71

---

READS

16

## 1 AUTHOR:



Zhaohui Li

University of Wisconsin - Parkside

159 PUBLICATIONS 3,176 CITATIONS

SEE PROFILE

# Sorption Kinetics of Hexadecyltrimethylammonium on Natural Clinoptilolite

Zhaohui Li\*

Geology Department and Chemistry Department, University of Wisconsin–Parkside,  
900 Wood Road, Box 2000, Kenosha, Wisconsin 53141-2000

Received October 29, 1998. In Final Form: May 21, 1999

Sorption kinetics of hexadecyltrimethylammonium (HDTMA) chloride on a natural clinoptilolite was studied in this research. The amount of HDTMA sorbed is a function of the initial HDTMA input and the sorption time. When the initial HDTMA input is less than the external cation-exchange capacity of the clinoptilolite, the HDTMA sorption is fast and equilibrium can be established in 1 h. As the initial HDTMA input is greater than the external cation-exchange capacity of clinoptilolite, which will result in more than a monolayer HDTMA surface coverage, the time for HDTMA sorption to reach equilibrium increases exponentially. The HDTMA sorption maximum on clinoptilolite increases logarithmically with mixing time. The counterion solution concentration data suggest that at the initial stage HDTMA molecules sorb on the zeolite via micelle forms, which is manifested by a decrease in chloride solution concentration with time. When HDTMA solution concentration is depleted to less than its critical micelle concentration, the adsorbed micelles (admicelles) rearrange themselves to a more stable monolayer or bilayer configuration, which is reflected by an increase in counterion solution concentration due to the desorption of chloride from admicelles. The time required for the surface rearrangement increases exponentially as the HDTMA input increases. The data of HDTMA sorption kinetics were fitted to different kinetic models, and the parabolic diffusion model fits the data best for the HDTMA sorption, counterion sorption at the initial stage, and counterion desorption at the rearrangement stage. Thus, the sorption of HDTMA on clinoptilolite surfaces is diffusion controlled. The results also indicate that it is incomplete to discuss surfactant sorption without counterion concentration data.

## Introduction

Sorption of cationic surfactants from solution onto solid surfaces has experienced extensive study in recent years. Depending on the surface charge of the solid, the sorption of cationic surfactants can be divided into the following categories: sorption on solids with high surface charge density, including some clay minerals, mica, and zeolite, and sorption on solids with low surface charge density, such as silica.<sup>1–2</sup> Several mechanisms, including ion exchange, ion pairing, acid–base interaction, polarization of  $\pi$  electrons, dispersion force, and hydrophobic bonding, were attributed to the sorption of cationic surfactants onto solid surfaces. Among them, ion exchange and hydrophobic bonding were the important ones.<sup>2–3</sup>

Sorption of cationic surfactants on a hydrophilic silica surface at low surface coverage revealed a two-step character with the first sorption plateau corresponding to the isoelectric point on the electrophoretic curve and the second plateau to twice the first plateau.<sup>4</sup> During the first step at low surface coverage, surfactant cations sorb physically as individual ions on the negatively charged surface sites. The sorbed surfactant cations with alkyl chains orienting toward the solution act as nucleation centers for surface aggregates to form through chain–chain association in the second step.<sup>5</sup> For surfaces with low charge density, a great increase in the chemical

potential of the solute in the bulk phase is necessary to initiate surface aggregation and, thus, the final structure is less compact.

On the other hand, sorption of cationic surfactants on materials with high surface charge density, such as zeolite and clay minerals, results in bilayer formation, provided that the initial surfactant concentration is greater than the critical micelle concentration (cmc) and the input surfactant is sufficient enough.<sup>6–8</sup> The counterions sorbed on the outer layer of the surfactant bilayer were readily exchanged following a lyotropic series.<sup>6</sup> When the initial surfactant concentration was less than the cmc, the surfactant molecules formed mainly a monolayer on zeolite surfaces, resulting in a greatly reduced chromate sorption.<sup>8</sup>

Recent studies on the properties of surfactant-modified zeolite (SMZ) indicate that it is an effective sorbent for multiple types of contaminants, such as chromate ions and perchloroethylene (PCE).<sup>6,8–11</sup> While the sorption of oxyanions by SMZ was attributed to anion exchange on the positively charged surfactant bilayer,<sup>6,8</sup> the sorption of hydrophobic organic contaminants was due to partitioning of the organics into the organic pseudophase created by the surfactant tail groups.<sup>10,11</sup> Sorption of PCE by SMZ at different surfactant surface coverages revealed that the surfactant surface configuration affected the PCE sorption coefficient to a great extent.<sup>11</sup>

\* Corresponding author. Phone: (414)595-2487. Fax: (414)595-2056. E-mail: li@uwp.edu.

(1) Rosen, M. J. *Surfactants and Interfacial Phenomena*, 2nd ed.; John Wiley & Sons: New York, 1989.

(2) Cases, J. M.; Villieras, F. *Langmuir* **1992**, *8*, 1251.

(3) Ingram, B. T.; Ottewill, R. H. In *Cationic Surfactants*; Rubingh, D. N., Holland, P. M., Eds.; Marcel Dekker: New York, 1991; Vol. 37, Chapter III, p 51.

(4) Zajac, J.; Trompette, J. L.; Partyka, S. *Langmuir* **1996**, *12*, 1357.

(5) Trompette, J. L.; Zajac, J.; Keh, E.; Partyka, S. *Langmuir* **1994**, *10*, 812.

(6) Li, Z.; Bowman, R. S. *Environ. Sci. Technol.* **1997**, *31*, 2407.

(7) Li, Z.; Bowman, R. S. *Environ. Eng. Sci.* **1998**, *15*, 237.

(8) Li, Z.; Anghel, I.; Bowman, R. S. *J. Dispersion Sci. Technol.* **1998**, *19*, 843.

(9) Haggerty, G. M.; Bowman, R. S. *Environ. Sci. Technol.* **1994**, *28*, 452.

(10) Bowman, R. S.; Haggerty, G. M.; Huddleston, R. G.; Neel, D.; Flynn, M. M. In *Surfactant-Enhanced Subsurface Remediation*; Sabatini, D. A., Knox, R. C., Harwell, J. H., Eds.; ACS Symposium Series 594; American Chemical Society: Washington, DC, 1995; p 54.

(11) Li, Z.; Bowman, R. S. *Environ. Sci. Technol.* **1998**, *32*, 2278.

Despite the importance of the structural arrangement of surfactant aggregates at the solid–liquid interface, information on this aspect is still limited.<sup>12</sup> Neutron reflection was used to measure the surfactant bilayer thickness on a quartz surface,<sup>13</sup> but the kinetics of how the bilayer formation was developed with respect to the initial surfactant concentration and the equilibration time was not addressed. Counterion effects on surfactant micelle formation have long been considered as an important aspect, but systematic studies of the interactions of counterions with surfactant surface aggregates have been ignored.<sup>14</sup> Without counterion information the study of surfactant sorption would yield only limited value.<sup>14</sup> Therefore, this study aims at monitoring the solution concentration changes for both the surfactant and the counterion. The time dependence of structural rearrangements of sorbed surfactant molecules with respect to different amounts of input surfactants will be studied from both surfactant sorption and counterion sorption. The relationship between the surfactant sorption maximum and the mixing time is determined. From the analysis of the amount of surfactant and counterions sorbed, the sorption kinetics of cationic surfactants on clinoptilolite is summarized.

### Experiments

Zeolite is a type of hydrous aluminosilicate belonging to tectosilicates in which the  $\text{SiO}_4$  tetrahedra form a 3-dimensional cage-like framework. In the zeolite structure, some  $\text{Si}^{4+}$  ions are replaced by  $\text{Al}^{3+}$ , which results in a net negative charge that needs to be balanced by exchangeable cations. Therefore, zeolite has cation-exchange capability and is commonly used as a cation exchanger. Clinoptilolite is a species of zeolite group minerals. The approximate chemical formula of clinoptilolite is  $(\text{Ca}, \text{Na}, \text{K})_6\text{Al}_6\text{Si}_{30}\text{O}_{72} \cdot 24\text{H}_2\text{O}$ . The dimensions of the open channels in clinoptilolite are  $0.89 \times 0.35 \text{ nm}^2$  for the 10-member ring and  $0.44 \times 0.30 \text{ nm}^2$  for the 8-member ring, large enough for a small exchangeable cation to enter and exit freely but too small for hexadecyltrimethylammonium (HDTMA) head groups. Thus, the sorption of HDTMA on clinoptilolite is only limited to the external cation-exchange sites.<sup>6</sup>

The clinoptilolite used in this study is from the St. Cloud mine in Winston, NM. The particle size of clinoptilolite aggregates ranges from 0.4 to 1.4 mm.  $\text{K}^+$  and  $\text{Ca}^{2+}$  are the major exchangeable cations. The clinoptilolite was used without pretreatment for HDTMA sorption. The initial HDTMA chloride (Aldrich, Milwaukee, WI) concentration was 20 mM. In each centrifuge tube (40-mL polyallomer) 10 mL of HDTMA aqueous solution was mixed with 8, 4, 2.67, 2, 1.5, 1.2, and 1 g of clinoptilolite, corresponding to initial inputs of 25, 50, 75, 100, 133, 167, and 200 mmol/kg. Since the external cation-exchange capacity (ECEC) of the clinoptilolite is about 100 mequiv/kg and the HDTMA sorption plateau is 200 mmol/kg,<sup>6</sup> the initial input encompassed sub-monolayer, full monolayer, partial bilayer, and full bilayer formations. The mixtures were shaken for varying amounts of time at 25 °C and 150 rpm on a shaker table and then centrifuged at 29100g for 15 min to yield a clear supernatant for HPLC analysis. When the mixing time was <15 min, the samples were filtered with 13-mm Gelman syringe filters. The separation time for filtration was about 5 s.

The HDTMA solution concentration was analyzed using an HPLC method with a Nucleosil CN column from Sigma-Aldrich (St. Louis, MO). The mobile phase was a mixture of 45% 5 mM *p*-toluenesulfonate aqueous solution and 55% methanol (v/v). A Waters 481 UV–vis detector was used, and the detection wavelength was 249 nm. At a flow rate of 1.0 mL/min, the retention time was 3.3 min and the linear response range was from 0.03 to 20 mmol/L.

The chloride concentration was also analyzed by HPLC with a Vydac 302IC ion chromatography column from the Separations Group (Hesperia, CA). The mobile phase was a 3 mM potassium hydrogen phthalate aqueous solution with pH 4.4 adjusted with 1 M NaOH. Detection was performed with a Waters 431 conductivity detector. At a flow rate of 2.0 mL/min, the retention time was 2.2 min and the linear response range was from 0.02 to 20 mmol/L.

All experiments were performed in duplicate, and standard curves were fitted on the basis of six standards with the linear coefficient of determination ( $r^2$ )  $\geq 0.999$ . The amount of HDTMA and counterion sorbed was calculated from the difference between the initial and final solution concentrations.

### Kinetic Models

Different kinetic models were used to describe sorption and desorption of ions from soils and soil minerals.<sup>15–17</sup> The goodness of fit of models is expressed by the coefficient of determination ( $r^2$ ). A relatively higher  $r^2$  value for the relationship between measured and predicted sorption and desorption data indicated that the model successfully described the kinetics of sorption and desorption.<sup>15</sup> But a high  $r^2$  value for a particular model does not necessarily mean that this model is the best.<sup>16</sup> Therefore, models producing  $r^2$  values  $>0.90$  for most treatment levels are used for discussion, and they are described below.

**First-Order Kinetic Model.** First-order kinetic models have been applied extensively to cation and anion sorption in soils. The first-order rate model for the sorption process can be expressed as<sup>15</sup>

$$\ln\left(1 - \frac{S_t}{S_m}\right) = -kt \quad (1)$$

where  $S_t$  is the amount of solute sorbed at time  $t$ ,  $S_m$  is the maximum amount of solute sorbed at equilibrium, and  $k$  is the apparent sorption rate constant. Similar to the case for sorption, the first-order rate model for desorption is<sup>15</sup>

$$\ln\left(\frac{S_t}{S_0}\right) = -k_d t \quad (2)$$

where  $S_0$  is the amount of solute sorbed at zero time of desorption and  $k_d$  is the apparent desorption rate constant. If the rate of HDTMA sorption by the clinoptilolite follows first-order kinetics, a plot of  $\ln(1 - S_t/S_m)$  against the sorption time  $t$  should yield a linear relationship.

**Parabolic Diffusion Model.** The parabolic diffusion law or equation can be used to determine whether diffusion-controlled phenomena are rate limiting. Parabolic diffusion was used to address the kinetics of sorption and reaction on soil constituents<sup>16</sup> and in the study of  $\text{NH}_4^+$  sorption on zeolite.<sup>15</sup> The parabolic diffusion model can be written as<sup>15,16</sup>

$$\frac{S_t}{S_m t} = kt^{-0.5} + a \quad (3)$$

and for desorption, the parabolic diffusion model is

(12) Huang, L.; Somasundaran, P. *Colloids Surf., A: Physicochem. Eng. Aspects* **1996**, *117*, 235.

(13) McDermott, D. C.; McCarney, J.; Thomas, R. K.; Rennie, A. R. *J. Colloid Interface Sci.* **1994**, *152*, 304.

(14) Bitting, D.; Harwell, J. H. *Langmuir* **1987**, *3*, 500.

(15) Kithome, M.; Paul, J. W.; Lavkulich, L. M.; Bomke, A. A. *Soil Sci. Soc. Am. J.* **1998**, *62*, 622.

(16) Sparks, D. L. *Kinetics of Soil Chemical Processes*; Academic Press: San Diego, CA, 1989.

(17) Chien, S. H.; Clayton, W. R. *Soil Sci. Soc. Am. J.* **1980**, *44*, 265.

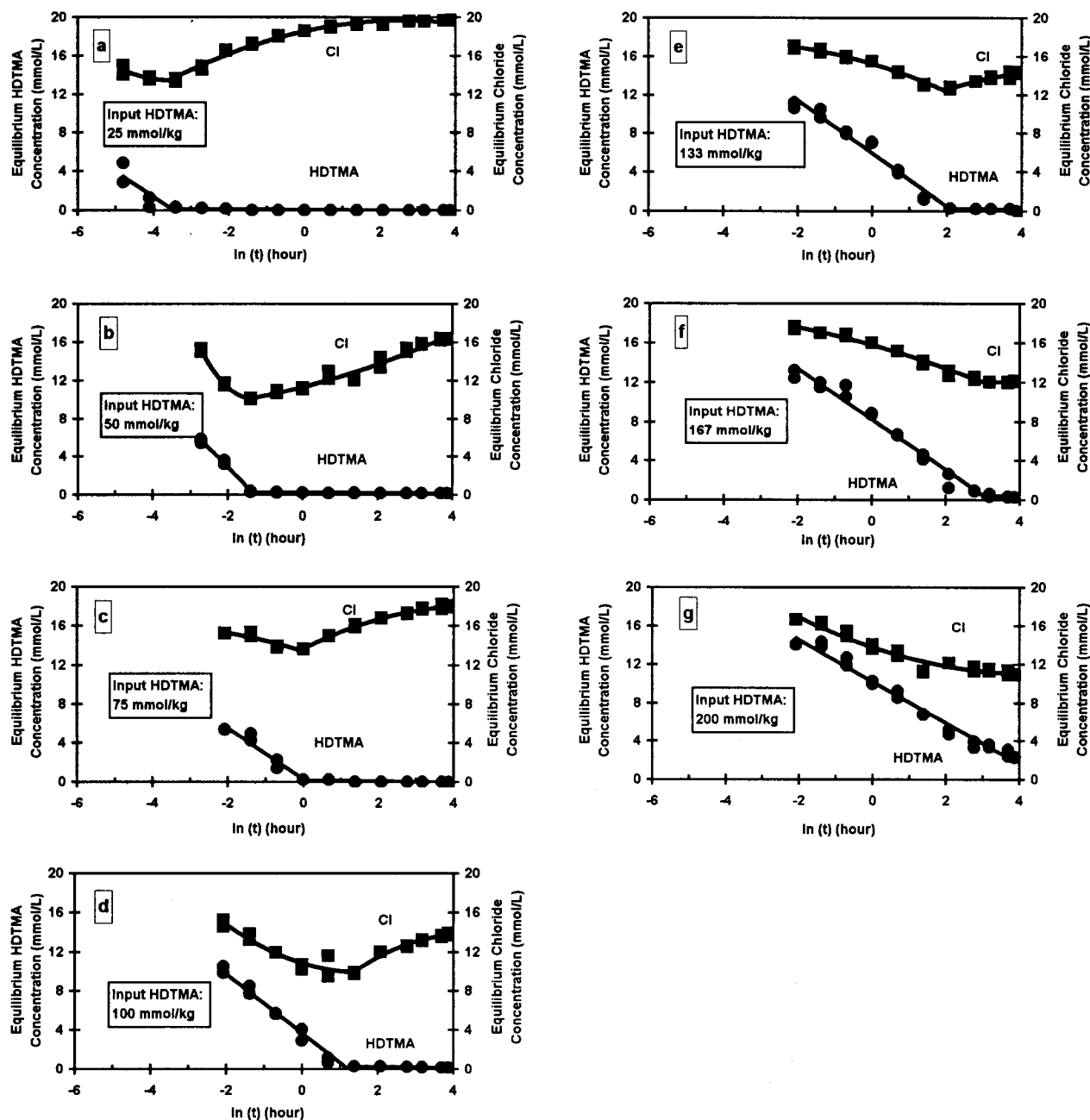


**Figure 1.** Equilibrium aqueous HDTMA (●) and chloride (■) concentrations versus sorption time when the initial input was 25 mmol/kg (a), 50 mmol/kg (b), 75 mmol/kg (c), 100 mmol/kg (d), 133 mmol/kg (e), 167 mmol/kg (f), and 200 mmol/kg (g).

$$\left(1 - \frac{S_t}{S_0}\right) \frac{1}{t} = k_d t^{-0.5} + a \quad (4)$$

where  $a$  is a constant and  $k$  is the overall diffusion constant for sorption and  $k_d$  is that for desorption.<sup>15</sup>

**Modified Freundlich Model.** The modified Freundlich model can be written as<sup>15,16</sup>

$$S_t = k C_0 t^a \quad (5)$$

in which  $a$  is a constant and  $C_0$  is the initial concentration of the solute. In this study, the input concentration was held constant while the amount of sorbent varied. So,  $C_0$  is the initial input. For desorption, the modified Freundlich model will be

$$S_0 - S_t = k_d S_0 t^a \quad (6)$$

**Elovich Model.** The Elovich model was used to study the sorption of phosphate on soil<sup>17</sup> and the sorption of  $\text{NH}_4^+$  on zeolite.<sup>15</sup> The Elovich model can be written as<sup>15,16</sup>

$$S_t = a \ln(t) + b \quad (7)$$

The Elovich model for desorption is

$$S_0 - S_t = a \ln(t) + b \quad (8)$$

In eqs 7 and 8,  $a$  and  $b$  are constants but their chemical significance is not clearly resolved.<sup>16</sup>

**Langmuir Sorption Isotherm.** Sorption of cationic surfactants on clinoptilolite follows the Langmuir sorption isotherm<sup>7-9</sup>

$$S_t = \frac{K_L S_m C}{1 + K_L C} \quad (9)$$

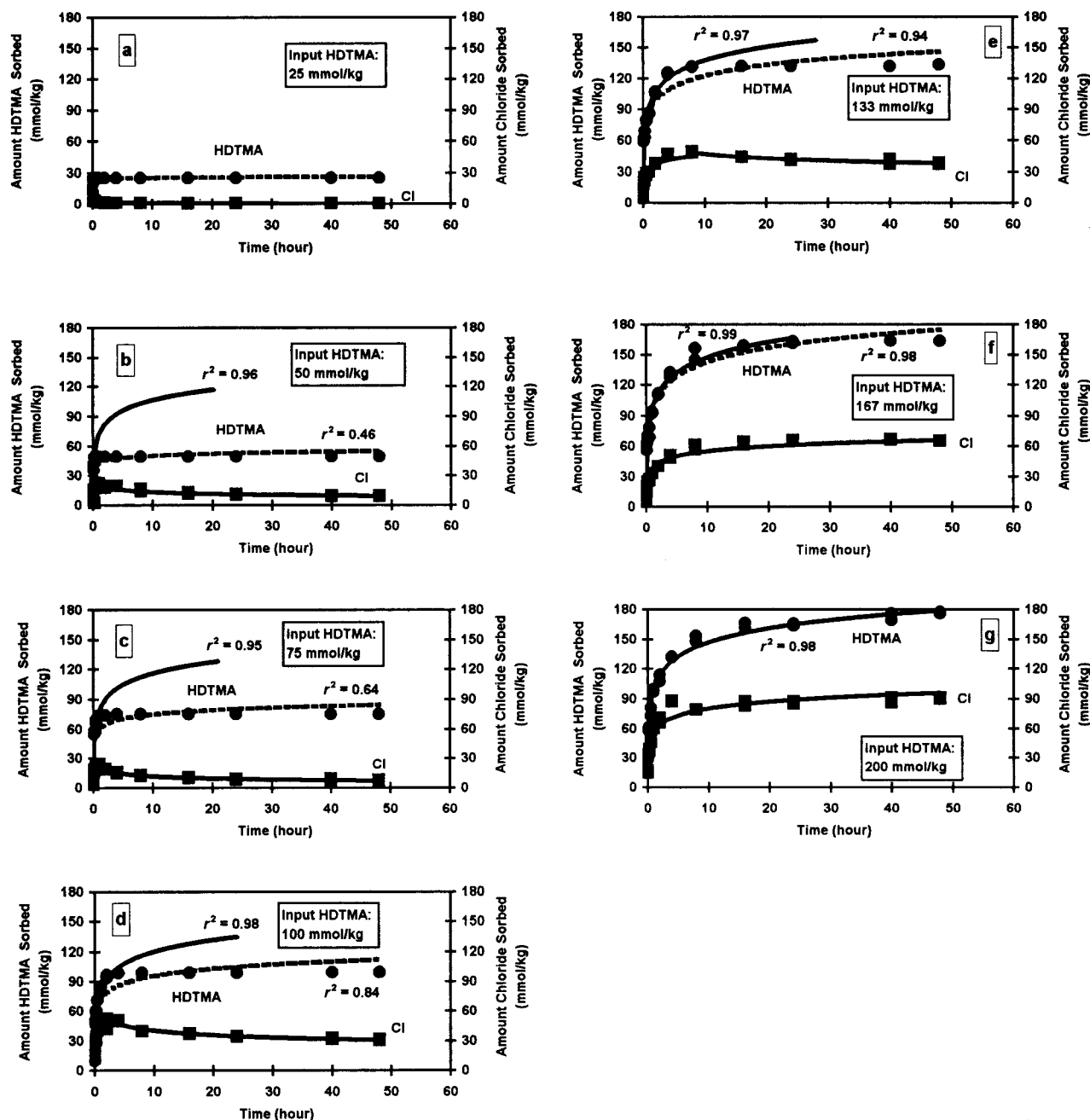


**Figure 2.** Amount of HDTMA (●) and chloride (■) sorbed with time when the initial input was 25 mmol/kg (a), 50 mmol/kg (b), 75 mmol/kg (c), 100 mmol/kg (d), 133 mmol/kg (e), 167 mmol/kg (f), and 200 mmol/kg (g). For HDTMA sorption, the dashed lines were fitted to the entire data and the solid lines were fitted to the data when surface rearrangement begins. Chloride sorption was fitted to the time when surface rearrangement begins, and desorption was fitted thereafter.

where  $C$  is the solute concentration in the liquid phase and  $K_L$  is the Langmuir sorption coefficient (L/kg). Equation 9 can be rearranged to

$$\frac{C}{S_t} = \frac{1}{K_L S_m} + \frac{C}{S_m} \quad (10)$$

Thus,  $K_L$  and  $S_m$  can be solved by linear regression of  $C/S_t$  versus  $C$ .

## Results

**Changes in HDTMA and Counterion Solution Concentrations with Time.** HDTMA and chloride solution concentrations versus sorption time for different surfactant surface coverages can be seen in Figure 1. When the data were plotted as  $\ln(\hat{t})$  versus solution concentration,

a clear trend could be seen for all the surface coverages. After the sorption takes place, both HDTMA and chloride solution concentrations start to decrease as the sorption time increases. When the initial input of HDTMA corresponds to less than a complete bilayer coverage, as represented in Figure 1a–f, the HDTMA solution concentration data show a transition time, beyond which the HDTMA solution concentration is depleted to less than the cmc (1.2 mmol/L). The counterion data also indicate a transition time, beyond which the counterion solution concentration starts to increase. These two transition times fall into the same time lapse, indicating a structural rearrangement of the sorbed surfactant molecules. However, the transition time is different for different initial HDTMA inputs. As HDTMA inputs increase, the transition time increases.



**Table 1. Rate Constants and Coefficients of Determination Based on Different Kinetic Equations for HDTMA Sorption**

kinetic equation	initial HDTMA input (mmol/kg)						
	25	50	75	100	133	167	200
first-order $k$ ( $\text{h}^{-1}$ )	$k = 40$ $r^2 = 0.59$	$k = 16$ $r^2 = 0.98$	$k = 3.7$ $r^2 = 0.98$	$k = 1.0$ $r^2 = 0.96$	$k = 0.5$ $r^2 = 0.99$	$k = 0.14$ $r^2 = 0.92$	$k = 0.08$ $r^2 = 0.92$
parabolic diffusion $k$ ( $\text{h}^{-0.5}$ ) and constant $a$	$k = 2.71$ $a = -0.91$ $r^2 = 0.93$	$k = 2.38$ $a = -0.75$ $r^2 = 0.96$	$k = 2.04$ $a = -0.61$ $r^2 = 0.96$	$k = 1.58$ $a = -0.68$ $r^2 = 0.98$	$k = 1.27$ $a = -0.34$ $r^2 = 0.96$	$k = 1.04$ $a = -0.32$ $r^2 = 0.96$	$k = 0.95$ $a = -0.23$ $r^2 = 0.96$
modified Freundlich $k$ ( $\text{h}^{-a}$ )	$a = 0.254$ $k = 2.72$ $r^2 = 0.78$	$a = 0.324$ $k = 1.61$ $r^2 = 0.99$	$a = 0.155$ $k = 0.99$ $r^2 = 0.95$	$a = 0.209$ $k = 0.79$ $r^2 = 0.96$	$a = 0.200$ $k = 0.68$ $r^2 = 0.98$	$a = 0.207$ $k = 0.55$ $r^2 = 0.97$	$a = 0.197$ $k = 0.45$ $r^2 = 0.95$
Elovich	$a = 2.06$ $b = 31.1$ $r^2 = 0.64$	$a = 14.9$ $b = 72.2$ $r^2 = 0.96$	$a = 9.88$ $b = 73.9$ $r^2 = 0.95$	$a = 15.1$ $b = 81.3$ $r^2 = 0.98$	$a = 18.4$ $b = 93.6$ $r^2 = 0.97$	$a = 21.7$ $b = 97.7$ $r^2 = 0.98$	$a = 21.6$ $b = 97.6$ $r^2 = 0.98$

**Table 2. Rate Constants and Coefficients of Determination Based on Different Kinetic Equations for Chloride Sorption during the Initial Admicelle Sorption Stage**

kinetic equation	initial HDTMA input (mmol/kg)						
	25	50	75	100	133	167	200
first-order $k$ ( $\text{h}^{-1}$ )	$k = 19$ $r^2 = 0.57$	$k = 8.7$ $r^2 = 0.96$	$k = 2.4$ $r^2 = 0.91$	$k = 0.46$ $r^2 = 0.60$	$k = 0.22$ $r^2 = 0.91$	$k = 0.10$ $r^2 = 0.92$	$k = 0.05$ $r^2 = 0.65$
parabolic diffusion $k$ ( $\text{h}^{-0.5}$ ) and constant $a$	$k = 10.6$ $a = -33.8$ $r^2 = 0.97$	$k = 5.74$ $a = -13.0$ $r^2 = 0.95$	$k = 2.60$ $a = -1.84$ $r^2 = 0.98$	$k = 1.51$ $a = -0.61$ $r^2 = 0.99$	$k = 1.13$ $a = -0.45$ $r^2 = 0.97$	$k = 0.86$ $a = -0.25$ $r^2 = 0.97$	$k = 1.01$ $a = -0.24$ $r^2 = 0.98$
modified Freundlich $k$ ( $\text{h}^{-a}$ )	$a = 0.128$ $k = 0.52$ $r^2 = 0.58$	$a = 0.143$ $k = 0.52$ $r^2 = 0.60$	$a = 0.157$ $k = 0.32$ $r^2 = 0.86$	$a = 0.195$ $k = 0.42$ $r^2 = 0.84$	$a = 0.226$ $k = 0.24$ $r^2 = 0.98$	$a = 0.234$ $k = 0.20$ $r^2 = 0.98$	$a = 0.278$ $k = 0.29$ $r^2 = 0.98$
Elovich	$a = 0.95$ $b = 11.5$ $r^2 = 0.6$	$a = 5.38$ $b = 30.9$ $r^2 = 0.80$	$a = 3.27$ $b = 24.3$ $r^2 = 0.87$	$a = 7.33$ $b = 43.2$ $r^2 = 0.86$	$a = 7.35$ $b = 33.3$ $r^2 = 0.96$	$a = 9.29$ $b = 36.3$ $r^2 = 0.97$	$a = 9.69$ $b = 57.9$ $r^2 = 0.90$

**HDTMA and Counterion Sorption with Time.** The amount of HDTMA and counterion sorbed at different times can be seen in Figure 2. In Figure 2, the HDTMA sorption data were fitted to the entire data range (dashed lines) by the Elovich model. The  $r^2$  values are relatively low when the initial input of HDTMA is less the ECEC. When the HDTMA sorption data were fitted only to the transition time (solid lines), the  $r^2$  values increased to  $>0.95$ . The  $r^2$  values from both fits again indicate that the transition time is important. Thus, the regressions for all the models were fitted to the data up to the transition time for each treatment. Their  $r^2$  values and apparent rate constants are listed in Table 1. The  $r^2$  values for HDTMA sorption based on the first-order kinetic model, the modified Freundlich model, the Elovich model, and the parabolic diffusion model were  $>0.9$  for all the treatment levels except the 25 mmol/kg surface coverage. The lower  $r^2$  values for the 25 mmol/kg surface coverage are due to fewer data points before the transition time is reached. The parabolic diffusion model had the best fit of the observed data at all surface coverage levels. In a study of  $\text{NH}_4^+$  sorption, the conformity to the parabolic diffusion model suggested that the process of  $\text{NH}_4^+$  sorption by the natural zeolite was diffusion controlled and that either intraparticle diffusion or surface diffusion may be rate limiting.<sup>15</sup> The head groups of HDTMA molecules are similar to  $\text{NH}_4^+$ . But three protons in  $\text{NH}_4^+$  are replaced by three methyl groups, and the fourth one is replaced by the tail group. The size of the HDTMA head group is too large to enter the zeolite channels for internal sorption sites. Thus, the sorption of HDTMA is limited to external cation-exchange sites on the zeolite surface. Since the clinoptilolite used is aggregated, intraparticle diffusion may be the predominant process for diffusion.

For chloride sorption, observed data points were fitted to the transition time for each treatment level. The  $r^2$  varied from 0.57 to 0.99 for most of the models except the parabolic diffusion, which produced  $r^2 > 0.95$  for all the initial HDTMA input (Table 2). Thus, counterion sorption data also indicate that diffusion was the primary factor

that governs the HDTMA sorption on zeolite surfaces. Beyond the transition time, since the HDTMA solution concentration is less than the cmc, further HDTMA sorption is limited and the counterions start to desorb, as manifested by increases in the aqueous chloride concentration (Figure 1). Therefore, desorption models were used to fit the observed data for chloride after the transition time. The results of apparent rate constants and  $r^2$  values are listed in Table 3. It can be seen from Table 3 that parabolic diffusion also provides the best fit. The rate constants for chloride desorption decrease as the input amount of HDTMA increases. The faster counterion desorption, when the input HDTMA is less than a monolayer coverage, indicates that monolayer HDTMA sorption on zeolite surfaces is more favorable.

**Apparent Rate Constants versus Initial Inputs.** For HDTMA sorption, the apparent rate constants for the first-order kinetic model decrease systematically as the HDTMA treatment level increases (Figure 3a). The values of  $a$  of the Elovich model increase logarithmically as the HDTMA treatment level increases (Figure 3a). The values of  $k$  from the parabolic diffusion and modified Freundlich models also decrease systematically as the HDTMA treatment level increases (Figure 3b). Similar results were found for  $\text{NH}_4^+$  sorption on clinoptilolite.<sup>15</sup> For chloride sorption, the apparent rate constants for the first-order kinetic, parabolic diffusion, and modified Freundlich models and the  $a$  value for the Elovich model follow the same trend as that with HDTMA sorption (Figure 3). The trend of the  $a$  value of the Elovich model indicates that its reciprocal may somehow be related to the rate constant.

The ratio of HDTMA sorbed to chloride sorbed versus different initial HDTMA inputs can be seen in Figure 4. When the HDTMA surface coverage is 25 mmol/kg, the ratio of HDTMA to counterion sorbed at 48 h was 60, indicating that only a monolayer exists or that the initial sorbed admicelles have already rearranged into a monolayer. The ratio decreased to about 10 for the 75 mmol/kg surface coverage. When the initial HDTMA input was equivalent to 200 mmol/kg surface coverage, the HDTMA

**Table 3. Rate Constants and Coefficients of Determination Based on Different Kinetic Equations for Chloride Desorption during the Surface Rearrangement Stage**

kinetic equation	initial HDTMA input (mmol/kg)				
	25	50	75	100	133
first-order $k$ ( $\text{h}^{-1}$ )	$k_d = 0.04$ $r^2 = 0.70$	$k_d = 0.02$ $r^2 = 0.86$	$k_d = 0.02$ $r^2 = 0.78$	$k_d = 0.006$ $r^2 = 0.95$	$k_d = 0.004$ $r^2 = 0.71$
parabolic diffusion $k$ ( $\text{h}^{-0.5}$ ) and constant $a$	$k_d = 1.62$ $a = -0.46$ $r^2 = 0.97$	$k_d = 0.21$ $a = -0.019$ $r^2 = 0.95$	$k_d = 0.20$ $a = -0.012$ $r^2 = 0.98$	$k_d = 0.12$ $a = -0.009$ $r^2 = 0.996$	$k_d = 0.06$ $a = -0.002$ $r^2 = 0.93$
modified Freundlich $k$ ( $\text{h}^{-a}$ )	$a = 0.08$ $k_d = 0.76$ $r^2 = 0.84$	$a = 0.37$ $k_d = 0.18$ $r^2 = 0.95$	$a = 0.31$ $k_d = 0.23$ $r^2 = 0.97$	$a = 0.27$ $k_d = 0.16$ $r^2 = 0.98$	$a = 0.53$ $k_d = 0.04$ $r^2 = 0.89$
Elovich	$a = 0.6$ $b = 7.7$ $r^2 = 0.89$	$a = 2.6$ $b = 7$ $r^2 = 0.87$	$a = 3.5$ $b = 4.6$ $r^2 = 0.96$	$a = 5.1$ $b = 4$ $r^2 = 0.98$	$a = 5.7$ $b = -5.2$ $r^2 = 0.90$

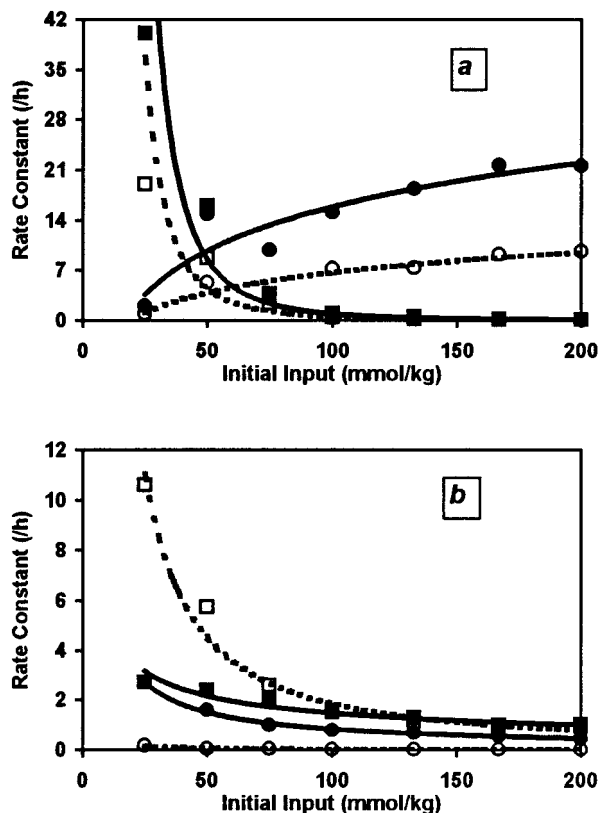


**Figure 3.** (a) Apparent rate constant for HDTMA sorption based on the first-order kinetic model (■) and the slopes  $a$  for the Elovich model (●). Apparent rate constants for chloride sorption based on the first-order kinetic model (□) and the slopes  $a$  for the Elovich model (○). Solid and dashed lines are based on logarithmic regression for the Elovich model and power function regression for the first-order kinetic model. (b) Apparent rate constants for HDTMA sorption based on the parabolic diffusion model (■) and the modified Freundlich model (●). Apparent rate constants for chloride sorption based on the parabolic diffusion model (□) and the modified Freundlich model (○). All lines are power function regressions with respect to model parameters.

sorption reached a maximum of 180 mmol/kg and the ratio of HDTMA to counterion sorbed decreased to 2, implying a complete bilayer formation on zeolite surfaces. On the other hand, if the ratio of HDTMA sorbed to counterion sorbed was plotted against the initial HDTMA input at the transition time when the surface rearrangement starts, the ratio remains approximately 2 regardless of the initial input (Figure 4). This value clearly indicates that the HDTMA sorbed before the rearrangement stage is in micelle forms. The same conclusion was reached in the study of HDTMA sorption on a mica surface when the initial HDTMA concentration was well above the cmc,

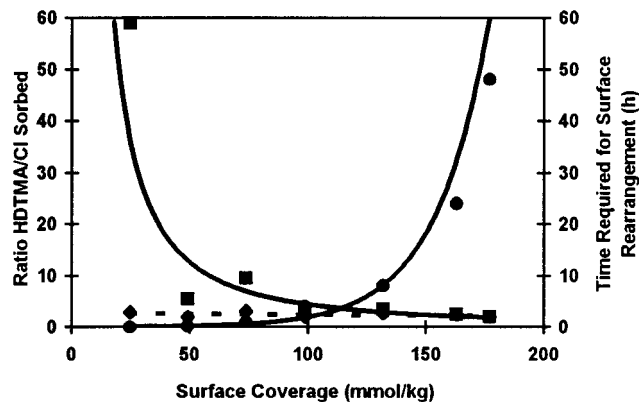


**Figure 4.** Time when surface rearrangement begins, which increases exponentially with input HDTMA (● with right  $y$ -axis) and ratios of HDTMA to chloride sorbed after 48 h of equilibrium (■ with left  $y$ -axis). However, the ratio remains almost constant (~2–2.5) at the time when surface rearrangement starts (◆ with the dash line).

and this phenomenon was attributed to a greater affinity of HDTMA micelles for the surface.<sup>18</sup> At the admicelle sorption stage, half of the positive charge of a micelle is balanced by the negative charge on zeolite surfaces and the other half is balanced by the counterion.

Given the ECEC of the clinoptilolite, the time required for surface rearrangement is a function of initial surfactant input (Figure 4). The time required for monolayer coverage is much less than that required for bilayer coverage. This fact was also observed in a study of HDTMA sorption on mica surfaces.<sup>18</sup>

**HDTMA Sorption Isotherms versus Initial HDTMA Inputs.** The HDTMA sorption isotherms at different mixing times can be seen in Figure 5. The fitted Langmuir parameters for each curve can be seen in Table 4 as well as Figure 6. The sorption maximum increases logarithmically as the mixing time increases. On the other hand, the Langmuir sorption coefficients, which reflect the relative affinity of the solute for the solid surface, decrease logarithmically as the mixing time increases. These results also show that monolayer sorption due to surface cation exchange is a fast step, while the bilayer sorption due to hydrophobic bonding requires much more time to reach equilibrium.

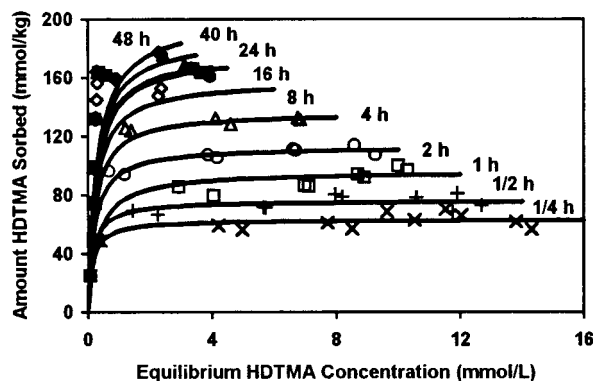
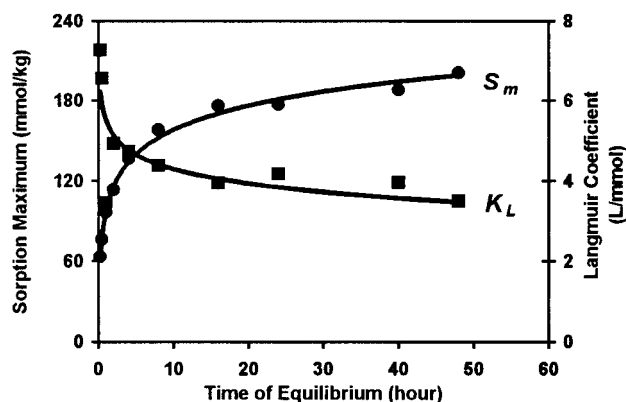
## Discussion

The cmc of HDTMA chloride is 1.2 mM while the initial HDTMA concentration is much greater than the cmc. Thus, the majority of the dissolved HDTMA molecules associate into normal micelles in aqueous solution. Due

(18) Chen, Y. L.; Chen, S.; Frank, C.; Israelachvili, J. *J. Colloid Interface Sci.* **1992**, *153*, 244.

**Table 4. Fitted Langmuir Parameters for HDTMA Sorption by Zeolite at Different Mixing Time**

parameter	48 h	40 h	24 h	16 h	8 h	4 h	2 h	1 h	1/2 h	1/4 h
$K_L$ (L/kg)	3.49	3.95	4.16	3.94	4.38	4.72	4.92	3.45	6.56	7.27
$S_m$ (mmol/kg)	201	188	177	176	158	136	113	96.4	76.3	63.4
$r^2$	0.95	0.97	0.98	0.98	0.993	0.998	0.999	0.993	0.990	0.98

**Figure 5.** HDTMA sorption isotherms at different mixing times. The lines are calculated from Langmuir fits to the observed data.**Figure 6.** Changes in sorption maximum (● with left y-axis) and Langmuir sorption coefficients (■ with right y-axis) with mixing time.

to the electrostatic interaction between the negatively charged zeolite surfaces and positively charged HDTMA micelles, the HDTMA micelles have a tendency to escape from water and sorb onto the solid surface. At the same time, the head group of the HDTMA monomers also interacts with zeolite surfaces due to the electrostatic interaction. Discrepancies regarding whether the initial sorption is in micelle form or monomer form have been seen in the literature. As pointed out by Kabalnov and Weers,<sup>19</sup> micelles cannot sorb directly on a solid surface, and when the initial surfactant concentration is greater than the cmc, the surfactant molecules associated in micelle form will first dissociate into monomers before being sorbed. However, calculation of the interaction energy indicates greater interaction energy between HDTMA micelles and a mica surface than between HDTMA monomers and a mica surface.<sup>18</sup> Looking at just the HDTMA sorption kinetic data is insufficient to determine whether the sorption of HDTMA onto zeolite surfaces was due to direct micelle attachment, so that admicelles form first, or only HDTMA monomers interact with zeolite surfaces and the depletion of HDTMA monomers was compensated by simultaneous dissociation of HDTMA micelles. The HDTMA sorption data only indicate that in aqueous solution HDTMA monomers are

more stable than HDTMA micelles. In other words, when the input HDTMA is less than twice the ECEC of the clinoptilolite, the HDTMA solution concentration never exceeds the cmc. Thus, no micelles are present in solution after the transition time. When the HDTMA solution concentration decreases to less than the cmc, the transfer of HDTMA molecules onto the zeolite surface becomes negligible (Figure 1). The counterion solution concentration data indicate that the HDTMA sorption involves two steps. The first is the fast sorption step, during which the micelles attach themselves directly on the zeolite surface. If the sorbed HDTMA molecules were in monomer form in this step, there should have been no changes in the counterion solution concentration. Thus, the decrease in the HDTMA solution concentration accompanying a simultaneous decrease in the counterion concentration at the initial stage should be explained as a process that involves removal of HDTMA micelles from the solution onto the solid surfaces. This result is directly opposite to the assumption used in a study of kinetics of mass transfer in surfactant sorption.<sup>19</sup> Due to the electrostatic interaction between the HDTMA head groups and the counterions, the counterions are initially sorbed onto the zeolite surface together with the HDTMA micelles. Such direct attachment of HDTMA micelles onto the zeolite surface resulted in admicelle (adsorbed micelle) formation on the surface. This stage is quasi stable due to the following facts. First, when the input HDTMA is less than the ECEC, more surface area is available than the HDTMA molecules can occupy. Therefore, in the second stage, the admicelles break apart and readjust themselves into an incomplete monolayer formation (Figure 7a and b). Second, when the input HDTMA is more than the ECEC and less than twice the ECEC of the solid, the amount of HDTMA molecules is more than enough to cover the whole zeolite surface with a monolayer. But the initial admicelle sorption will prevent admicelles from overlapping each other, leaving part of the surface uncovered (Figure 7c). The second stage is the later rearrangement stage. The amount of HDTMA sorbed at the later stage does not increase significantly with time. This is because the HDTMA aqueous concentration is depleted to below the cmc. The filling of still available sorption sites by HDTMA molecules after the first fast sorption stage results in a breakdown of initially sorbed admicelles. This process will cause desorption of counterions from the surfaces and, thus, an increase in the counterion solution concentration, as represented by Figure 1d–f. The second stage can be depicted by the transition from Figure 7a to Figure 7b when the input HDTMA is less than the ECEC and the transition from Figure 7c to Figure 7d when the input HDTMA is greater than the ECEC. The rate constants for counterion sorption are much greater than that for counterion desorption, which is a direct indication that the admicelle sorption stage is fast and that the transition from admicelle to bilayer is the slower stage (Tables 2 and 3). A similar two-step sorption was observed in a study of HDTMA sorption on a mica surface.<sup>18</sup>

The data presented here represent the first use of the first-order kinetic, modified Freundlich, parabolic diffusion, and Elovich rate models to describe the HDTMA and counterion sorption kinetics on natural clinoptilolite. No similar studies could be found in the literature, and

(19) Kabalnov, A.; Weers, J. *Langmuir* **1996**, *12*, 3342.



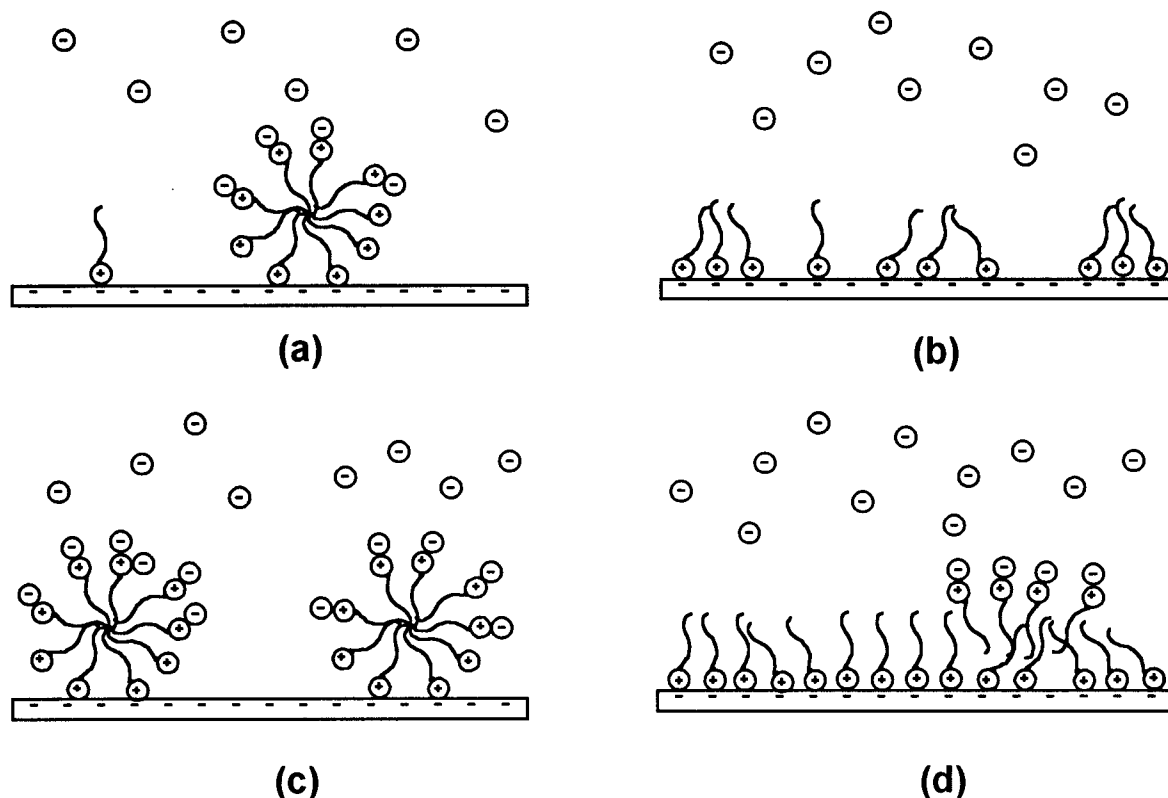


**Figure 7.** HDTMA sorption on a zeolite surface. Initial admicelle sorption when the amount of input HDTMA is less than the monolayer coverage (a). Later surface rearrangement of sorbed HDTMA molecules results in desorption of initially sorbed counterions (b). Initial admicelle sorption when the amount of input HDTMA is greater than the monolayer coverage (c). Later surface rearrangement of sorbed HDTMA molecules results in desorption of some of the initially sorbed counterions (d). The space between admicelles in (c) is not large enough to hold another admicelle. Later rearrangement allows the space to be filled with monomers so that a complete monolayer coverage can be achieved.

thus, it is difficult to compare the results. Nevertheless, The results in this study present a clear picture of HDTMA sorption on a highly charge solid surface by combining the HDTMA sorption data with counterion sorption data.

### Conclusions

From this study it can be concluded that the sorption of HDTMA on a high surface charged zeolite is a function of mixing time and initial surfactant input. The HDTMA sorption onto zeolite involves two stages. The first stage is due to direct attachment of HDTMA micelles onto the zeolite surface. The second stage is due to surfactant surface rearrangement, which results in a transition from admicelle to monolayer when the initial surfactant input is less than the ECEC or a transition from admicelle to incomplete bilayer when the surfactant input is less than twice the ECEC. While the first stage is fast, the second stage is a slow process involving intraparticle diffusion. The time when surface rearrangement begins depends on the initial surfactant input. The results indicate that equilibrium in terms of removal of HDTMA from aqueous

solution can be established when the HDTMA solution concentration is less than the cmc, but the true equilibrium in terms of no counterion desorption takes an extralong time. The results also show that counterion sorption/desorption data provide significant information regarding the surfactant surface configuration and, thus, should be included in studies of surfactant sorption. It is incomplete to discuss surfactant sorption without counterion data available.

**Acknowledgment.** This research was supported through the USDOE Federal Energy Technology Center under Contract #DE-AR21-95MC32108. The author thanks R. S. Bowman of New Mexico Tech for helpful discussions on data interpretation, constructive comments on manuscript writing, and instrument use. Stephen J. Roy, Shawn Williams, and Todd Burt of New Mexico Tech performed some of the experimental work. Constructive comments and helpful corrections of errors and mistakes by the reviewers are greatly appreciated.

LA981535X